Analysis of the Interference Due to Differential Rain Attenuation Induced by an Adjacent Path on a Triple-Site Diversity Earth-Space System

John D. Kanellopoulos, *Senior Member, IEEE,* and Spiros N. Livieratos

***Abstract*— The reliable design of satellite communication systems requires the consideration of interference effects. Interference caused by differential rain attenuation from an adjacent earth–space system is taken under consideration here. In particular, a method to predict rain differential attenuation statistics used for single/double site earth–space systems is extended to include triple-site diversity ones. The modified method is again based on a model of convective rain cells as well as on the lognormal assumption for the point rainfall rate distribution at the location under consideration. In an analogous fashion with the (C/N) ratio, a ≪(C/I) diversity gain≫ is also adopted here and some very useful remarks concerning the effectiveness of the triple-site diversity protection as a countermeasure technique are deduced. As a general conclusion, it can be stated that the triple-site scheme not only reduce the potential large attenuation margins significantly, but also leads to the establishment of the minimum separation between satellites operating under permitted interference levels.**

***Index Terms*— Attenuation, interference, propagation, rain, satellite communication.**

NOMENCLATURE

φ_i	Elevation angle of the slant paths pointing toward satellite S_i ($i = 1,2$).
θ_d	Differential angle between two satellites.
S_{ij}	Site separation between stations E_i and E_j ($i, j = 1,2,3, i \neq j$).
D_{ij}	Distance between the projections of the slant radio paths E_iS_1 and E_jS_1 ($i, j = 1,2,3, i \neq j$).
H	Effective rain height.
Λ	Latitude of the specific location.
H_o	Average height above sea level.
E	Mean radius of the earth.
A_{c_i}	Rain attenuations of the wanted signal referring to earth-space slant paths E_iS_i ($i = 1,2,3$).
A_{I_i}	Rain attenuations of the interfering signal referring to earth–space slant paths E_iS_2.
M	System margin available for rain attenuation.
$(C/I)_i$ ($i = 1,2,3$)	Carrier-to-interference ratio at the earth station E_i receiver.
$(C/I)_{i,\,\mathrm{nom}}$ ($i = 1,2,3$)	Carrier to interference ratio as above but under clear-sky conditions.
L_C	Effective average length of the earth-satellite paths corresponding to the wanted signal.
L_I	Effective average length of the earth-satellite paths corresponding to the interfering signal.
L_{CD}, L_{ID}	The projected L_C and L_I, respectively.
A'_{c_i}	Rain attenuations calculated for the projections of the slant paths E_iS_1 ($i = 1,2,3$).
A'_{I_i}	Rain attenuations calculated for the projections of the slant paths E_iS_2 ($i = 1,2,3$).
a, b	Constants of the specific rain attenuation A_o (in decibels/kilometer).
G	Characteristic distance modeling the spatial inhomogeneity of the rainfall structure.
D_r	Diameter of the rain cell size.
R_m, S_r	Lognormal statistical parameters of the point rainfall distribution.
r	Nonexceedance level of the (C/I) ratio (in decibels).
A_{m_1}, S_{a_1}	Lognormal statistical parameters of the distributions concerning A'_{c_1}, A'_{c_2}, A'_{c_3} $r.vs.$
A_{m_2}, S_{a_2}	Lognormal statistical parameters of the distributions concerning A'_{I_1}, A'_{I_2}, A'_{I_3} $r.vs.$
$f_{U_1U_2U_3}$	Three-dimensional normal joint density function.
$f_{U_iU_j}$	Two-dimensional normal joint density function ($i, j = 1,2,3, \quad i \neq j$).
μ_j, σ_j	Statistical parameters expressed in terms of the logarithmic
	($j = 1,2,3,4,5,6$) correlation coefficients $\rho_{n_{ij}}$($i, j = 1,2,3, i \neq j$) and $\rho_{n_{ik}}$ ($i = 1,2,3; k = 4,5,6$).

Manuscript received December 28, 1996; revised July 8, 1998.

The authors are with the Division of Electroscience, Department of Electrical Engineering, National Technical University of Athens, Zografou, Athens, 15773 Greece.

Publisher Item Identifier S 0018-926X(99)02488-6.

II. INTRODUCTION

FREQUENCIES above 10 GHz will be of high importance in future satellite systems as they will allow high-communication capacities. In this band of frequencies, how-

ever, attenuation caused by rain is a basic limiting factor affecting the performance of these systems, especially in heavy rain climatic regions, e.g., climatic zones F, H, K, L, M, N, P, Q. In such conditions and considering very large availability time specifications, the site-diversity configuration has been introduced as a mitigation technique to reduce the required large fade margins [1]–[5]. In some severe cases such as operation in the k_α band (30/20 GHz), the link margins result very large and consequently the double-site diversity protection can be proved to be inadequate leading to the employment of triple-site diversity [1]. This is more evident for earth–space paths located in subtropical/tropical regions where the imperative need for reliable transmission with low fade margins, as stated above, seems to impose the inevitable use of triple-site configuration. So far, a number of three-site diversity systems have been operated such as the most recent experiment at 20 GHz, which has been in near continuous operation since September 1994 [6].

Furthermore, interference effects—another important error inducing propagation mechanism—must be taken into account for the reliable design of a satellite communication system. The dominant interference source examined in this paper refers to interference caused by differential rain attenuation from an adjacent earth–space system operating at the same frequency. The lateral inhomogeneity in the precipitation medium may result in interference to the signal from the adjacent satellite. This type of interference is considered to be a very serious problem for the future satellite systems where orbital and frequency congestion is expected to be move restrictive.

So far, the analysis of this problem has been restricted to single site systems [7]–[9]. In a very recent publication, the double site diversity case has also been examined [10]. The subject of the present paper is the extension of the latter analysis to include interfered systems operating with triple-site diversity protection, which is indispensable in some cases, as stated above. From this point of view, the possibility of the present described scenario actually occurring seems not to be remote, particularly for earth–space paths located in subtropical/tropical regions. The extended method is based again on the same assumptions as before [8]–[10].

The numerical results taken by means of the proposed procedure are concentrated on the analytical examination of the carrier-to-interference ratio and the corresponding diversity gain in relation to the various parameters of the problem. Some very useful conclusions indicating the benefit of the satellite design process are drawn.

III. The Interference Analysis

The configuration of the present problem is shown in Fig. 1(a). Three earth–stations E_1, E_2, and E_3 are in communication with a satellite S_1, forming a triple-site diversity protection scheme. A second satellite S_2 operating at the same frequency is in orbit close to S_1; the two subtending an angle θ_d to E_1, E_2, and E_3. The slant paths corresponding to the wanted and potential interfering signals have generally different elevation angles given by φ_1 and φ_2, respectively [see also Fig. 1(a)]. For better information about the geometry of the problem one is referred elsewhere [8]. Note that the θ_d will be slightly different for each station E_1, E_2, and E_3. This angle can be analytically expressed in terms of the slant ranges between earth–station ith satellite ($i = 1, 2$) and the radius of the geostationary orbit [11]. Assuming now that the site separation distances $S_{i,j}$ ($i, j = 1, 2, 3$, $i \neq j$) between the ith and jth earth stations are very small compared to the various slant ranges and the geostationary orbit radius, it can be deduced that the difference between the θ_d's is negligible with approximation better than one per thousandth.

The following values of rain attenuation are important: A_{c_1}, A_{c_2}, A_{c_3} of the wanted signal referring to earth–space paths E_1S_1, E_2S_1, and E_3S_1, the corresponding ones A_{I_1}, A_{I_2}, A_{I_3} of the potential interfering signal along the paths E_1S_2, E_2S_2, E_3S_2, and the system margins M_1, M_2, M_3 available for rain attenuation. All these terms are, of course, expressed in decibels. A balanced diversity system, commonly used in practice, will be adopted here leading to the assumption $M_1 = M_2 = M_3 = M$.

As a result of the site-diversity scheme, the selection of the receiving station (E_1, E_2, or E_3) at each instant will depend on the carrier-to-noise plus interference ratios $(C/N)_1$, $(C/N)_2$, and $(C/N)_3$ levels, respectively. Following the reasonable assumption that a noise-dominant system in the presence of an interfering satellite transmitter is considered $(C/N < C/I)$ [11], the above selection criterion is almost equivalent to the consideration of the receiving earth station by means of switching to the least attenuated path.

Further, an outage of the wanted signal will occur whenever $A_{c_1} \geq M$, $A_{c_2} \geq M$, and $A_{c_3} \geq M$. For a noise-dominated system, the additive contribution of the interference effects on the total outage time can be taken into account by means of the following probability: this is the fraction of the time when the system suffers from interference as part of the total time when the event $A_{c_1} \geq M$, $A_{c_2} \geq M$, and $A_{c_3} \geq M$ is not valid, but the system is under rain fade conditions. In mathematical terms, this conditional probability, which is the main objective of the present analysis, can be expressed as

$$P = \frac{P_1 + P_2 + P_3}{P_4 + P_5 + P_6} \tag{1}$$

where

$$\left.\begin{aligned} P_1 &= P\left[\left(\frac{C}{I}\right)_1 \leq r,\ r_M \leq A_{c_1} \leq M,\ A_{c_1} \leq A_{c_2},\ A_{c_1} \leq A_{c_3}\right] \\ P_2 &= P\left[\left(\frac{C}{I}\right)_2 \leq r,\ r_M \leq A_{c_2} \leq M,\ A_{c_2} \leq A_{c_1},\ A_{c_2} \leq A_{c_3}\right] \\ P_3 &= P\left[\left(\frac{C}{I}\right)_3 \leq r,\ r_M \leq A_{c_3} \leq M,\ A_{c_3} \leq A_{c_1},\ A_{c_3} \leq A_{c_2}\right] \end{aligned}\right\} \tag{2}$$

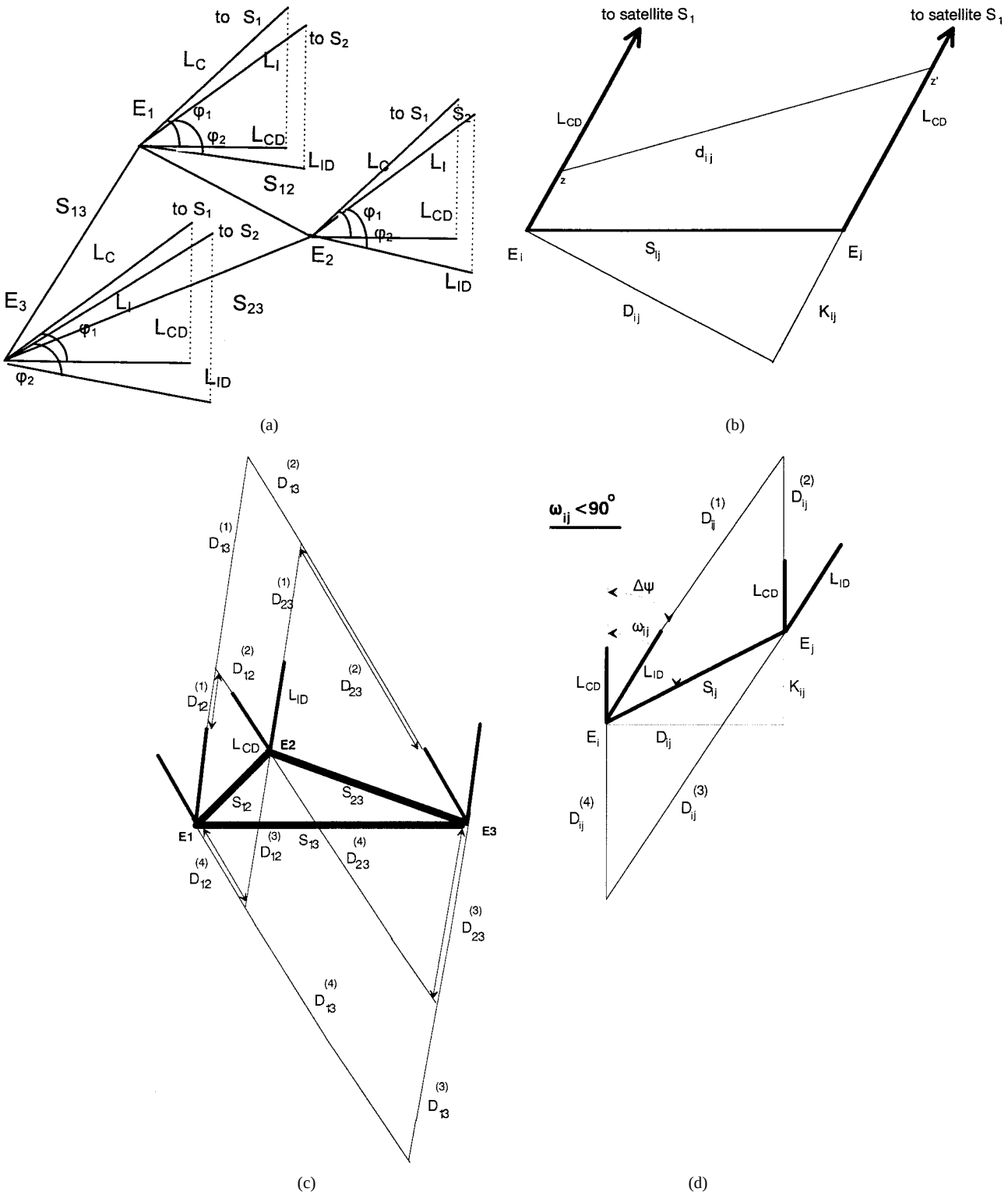

Fig. 1. (a) Configuration of the problem under consideration. (b) The projections of the slant paths corresponding to the earth–stations E_i and E_j, respectively. (c) Presentation of the lengths $D_{ij}^{(\ell)}$ as required for the calculation of the factors H_{ik} (Appendix B). (d) The lengths $D_{ij}^{(\ell)}$ for $\omega_{ij} < 90°$.

and

$$\left.\begin{aligned} P_4 &= P[r_M \le A_{c_1} \le M,\ A_{c_1} \le A_{c_2},\ A_{c_1} \le A_{c_3}] \\ P_5 &= P[r_M \le A_{c_2} \le M,\ A_{c_2} \le A_{c_1},\ A_{c_2} \le A_{c_3}] \\ P_6 &= P[r_M \le A_{c_3} \le M,\ A_{c_3} \le A_{c_1},\ A_{c_3} \le A_{c_2}] \end{aligned}\right\} \quad (3)$$

where $(C/I)_i$ $(i = 1,2,3)$ is the carrier-to-interference ratio at the input of E_ith receiver.

Under rain fade conditions, the above ratios are given by

$$\left(\frac{C}{I}\right)_i = \left(\frac{C}{I}\right)_{i,\,\mathrm{nom}} - A_{c_i} + A_{I_i} \qquad (i = 1,\ 2,\ 3) \quad (4)$$

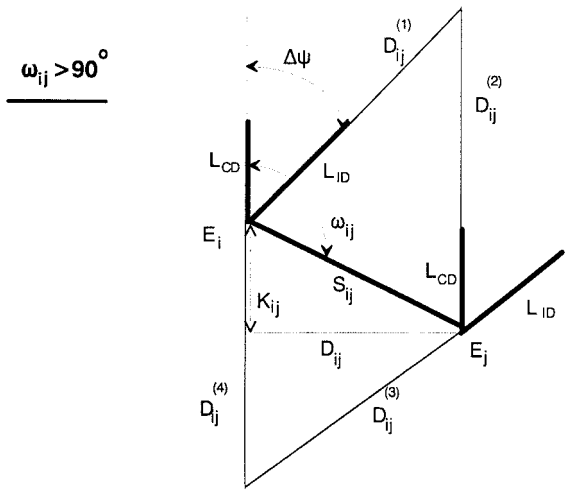

(e)

Fig. 1. (*Continued.*) (e) The lengths $D_{ij}^{(\ell)}$ for $\omega_{ij} > 90°$.

TABLE I
PARAMETERS OF THE INTERFERENCE PROBLEMS

Georgia	Tropical Region
$H = 4.3$ km	$H = 3.8$ km
$H_o = 0.1$ km	$H_o = 0.1$ km
$R_m = 0.04964$	$R_m = 0.13415$
$S_r = 1.8677$	$S_r = 1.8568$
$G = 1.75$ km	$G = 0.75$ km
19 GHz	19 GHz
$a = 0.077, b = 1.099$	$a = 0.075, b = 1.099$
28.5 GHz	28.5 GHz
$a = 0.187, b = 1.021$	$a = 0.187, b = 1.021$
$\varphi_1 = 29°, \varphi_2 = 29°$	$\varphi_1 = 29°, \varphi_2 = 29°$
$\theta_d = 4°, 6°, 8°$	$\theta_d = 4°, 6°, 8°$

where $(C/I)_{i,\,\mathrm{nom}}$ is the ratio, under nominal conditions (clear-sky conditions), concerning the ith station.

In addition, r is the nonexceeded carrier-to-interference ratio level, whereas the quantity r_M is an indicative threshold depending on the sensitivity of the attenuation measurements, used to describe the period of time where the system operates under rain fade conditions. The specific value "0.5" suggested by Rogers *et al.* [7] will be adopted here.

The derivation of (1)–(3) is a direct result of the Bayes theorem [12] and since the following conditions hold:

$$\left.\begin{aligned} P_1 &< P_4 \\ P_2 &< P_5 \\ P_3 &< P_6 \end{aligned}\right\} \tag{5}$$

the probability P in (1) will be always less than unity. More details concerning the derivation of (1)–(3) can be found in Appendix A.

A. General Considerations

The analysis that follows is based on a number of assumptions.

The lognormal form is adopted for both the unconditional (including nonraining time) point rainfall rate R and the rain attenuation A distributions [13].

The geometrical parameters for the satellite systems under consideration are the geographical longitudes of the two geostationary satellites θ_{S_1}, θ_{S_2} and their angular separation $\beta = |\theta_{S_1} - \theta_{S_2}|$. The elevation angles of the slant paths φ_1, φ_2, and the angular separation θ_d between the two satellites as seen by earth–station antenna can be expressed in terms of the above parameters θ_{S_1}, θ_{S_2}, and β [11]. The numerical values for φ_1, φ_2, θ_d concerning the systems under consideration, as presented in the third section of the paper, are tabulated in Table I.

According to Crane's considerations for the vertical variation of the rainfall structure [14], the rain structure from the ground up to an effective rain height H is assumed to be uniform given by

$$\left.\begin{aligned} H &= 4.8 \text{ km} && |\Lambda| \le 30° \\ H &= 7.8 - 0.1|\Lambda| \text{ km} && |\Lambda| > 30° \end{aligned}\right\} \tag{6}$$

where Λ is the latitude of the specific location in degrees. As a result, the effective average lengths of the earth-satellite paths corresponding to the wanted (L_C) and interfering (L_I) signals affected by rain are given by

$$\left.\begin{aligned} L_C &= \frac{H - H_o}{\sin \varphi_1} \\ L_I &= \frac{H - H_o}{\sin \varphi_2} \end{aligned}\right\} \quad \varphi_i \ge 10° \ (i = 1, 2) \tag{7}$$

$$\left.\begin{aligned} L_C &= [(E+H)^2 - (E+H_o)^2 \cos^2 \varphi_1]^{1/2} \\ &\quad - (E+H_o) \sin \varphi_1 \\ L_I &= [(E+H)^2 - (E+H_o)^2 \cos^2 \varphi_2]^{1/2} \\ &\quad - (E+H_o) \sin \varphi_2 \end{aligned}\right\} \quad \varphi_i < 10° \tag{8}$$

where E is the mean radius of the earth and H_o is the average height above sea level of the earth station.

Taking into account these considerations, we obtain the probabilities encountered in (1)–(3) as follows:

$$\begin{aligned} P_1 &= P\left[A_{I_1} \le A_{c_1} - \left(\left(\frac{C}{I}\right)_{1\,\mathrm{nom}} - r\right), \right. \\ &\qquad \left. 0.5 \le A_{c_1} \le M,\ A_{c_1} \le A_{c_2},\ A_{c_1} \le A_{c_3}\right] \\ &= P\left[\frac{A'_{I_1}}{\cos \varphi_2} \le \frac{A'_{c_1}}{\cos \varphi_1} - \left(\left(\frac{C}{I}\right)_{1\,\mathrm{nom}} - r\right), \right. \\ &\qquad \left. 0.5 \le \frac{A'_{c_1}}{\cos \varphi_1} \le M,\ A'_{c_1} \le A'_{c_2},\ A'_{c_1} \le A'_{c_3}\right] \end{aligned} \tag{9}$$

$$\begin{aligned} P_2 &= P\left[A_{I_2} \le A_{c_2} - \left(\left(\frac{C}{I}\right)_{2\,\mathrm{nom}} - r\right), \right. \\ &\qquad \left. 0.5 \le A_{c_2} \le M,\ A_{c_2} \le A_{c_1},\ A_{c_2} \le A_{c_3}\right] \\ &= P\left[\frac{A'_{I_2}}{\cos \varphi_2} \le \frac{A'_{c_2}}{\cos \varphi_1} - \left(\left(\frac{C}{I}\right)_{2\,\mathrm{nom}} - r\right), \right. \\ &\qquad \left. 0.5 \le \frac{A'_{c_2}}{\cos \varphi_1} \le M,\ A'_{c_2} \le A'_{c_1},\ A'_{c_2} \le A'_{c_3}\right] \end{aligned} \tag{10}$$

$$P_3 = P\left[A_{I_3} \le A_{c_3} - \left(\left(\frac{C}{I}\right)_{3\,\mathrm{nom}} - r\right),\ 0.5 \le A_{c_3} \le M,\ A_{c_3} \le A_{c_1},\ A_{c_3} \le A_{c_2}\right]$$
$$= P\left[\frac{A'_{I_3}}{\cos\varphi_2} \le \frac{A'_{c_3}}{\cos\varphi_1} - \left(\left(\frac{C}{I}\right)_{3\,\mathrm{nom}} - r\right),\ 0.5 \le \frac{A'_{c_3}}{\cos\varphi_1} \le M,\ A'_{c_3} \le A'_{c_1},\ A'_{c_3} \le A'_{c_2}\right] \quad (11)$$

$$\left.\begin{aligned} P_4 &= P\left[0.5 \le \frac{A'_{c_1}}{\cos\varphi_1} \le M,\ A'_{c_1} \le A'_{c_2},\ A'_{c_1} \le A'_{c_3}\right] \\ P_5 &= P\left[0.5 \le \frac{A'_{c_2}}{\cos\varphi_1} \le M,\ A'_{c_2} \le A'_{c_1},\ A'_{c_2} \le A'_{c_3}\right] \\ P_6 &= P\left[0.5 \le \frac{A'_{c_3}}{\cos\varphi_1} \le M,\ A'_{c_3} \le A'_{c_1},\ A'_{c_3} \le A'_{c_2}\right] \end{aligned}\right\}. \quad (12)$$

In these expressions, A'_{c_1}, A'_{c_2}, A'_{c_3}, and A'_{I_1}, A'_{I_2}, and A'_{I_3} are the rain attenuations calculated for hypothetical terrestrial links (the projections of the slant paths) with path lengths

$$\left.\begin{aligned} L_{CD} &= L_C \cos\varphi_1 \\ L_{ID} &= L_I \cos\varphi_2 \end{aligned}\right\}. \quad (13)$$

The specific rain attenuation (in dB/km), as a function of rainrate (in mm/h), is given by

$$A_o = aR^b \quad (14)$$

where the constants a and b depend on frequency, incident polarization, and the microstructure of the rain [15].

The convective raincell model proposed by Lin [16] (as modified by Kanellopoulos and Koukoulas [13]) will be used for the horizontal variation of the rainfall structure. According to this model, the spatial correlation coefficient ρ_o of specific rain attenuation between two points, being at a distance d in the rain medium is given by

$$\rho_o = \left\{\begin{aligned} &\frac{G}{\sqrt{G^2 + d^2}}, && \text{for } d < D_r \\ &\frac{G}{\sqrt{G^2 + D_r^2}}, && \text{for } d \ge D_r \end{aligned}\right\} \quad (15)$$

where G is a characteristic distance ranging from 0.75–3 km and D_r is the diameter of the raincells in the specific area.

B. Evaluation of the Conditional Probability

Following the previous considerations, the joint exceedance probabilities appearing in (9)–(12) can be evaluated as

$$P_1 = \int_{x_t}^{M\cos\varphi_1} dy_1 \int_{y_1}^{\infty} dy_2 \int_{y_1}^{\infty} dy_3 \cdot \int_{o}^{(\cos\varphi_2/\cos\varphi_1)y_1 - r'\cos\varphi_2} dy_4 \cdot f_{A'_{c_1}A'_{c_2}A'_{c_3}A'_{I_1}}(y_1, y_2, y_3, y_4) \quad (16)$$

$$P_2 = \int_{x_t}^{M\cos\varphi_1} dy_2 \int_{y_2}^{\infty} dy_1 \int_{y_2}^{\infty} dy_3 \cdot \int_{o}^{(\cos\varphi_2/\cos\varphi_1)y_2 - r'\cos\varphi_2} dy_5 \cdot f_{A'_{c_1}A'_{c_2}A'_{c_3}A'_{I_2}}(y_1, y_2, y_3, y_5) \quad (17)$$

$$P_3 = \int_{x_t}^{M\cos\varphi_1} dy_3 \int_{y_3}^{\infty} dy_1 \int_{y_3}^{\infty} dy_2 \cdot \int_{o}^{(\cos\varphi_2/\cos\varphi_1)y_3 - r'\cos\varphi_2} dy_6 \cdot f_{A'_{c_1}A'_{c_2}A'_{c_3}A'_{I_3}}(y_1, y_2, y_3, y_6) \quad (18)$$

$$P_4 = \int_{0.5\cos\varphi_1}^{M\cos\varphi_1} dy_1 \int_{y_1}^{\infty} dy_2 \int_{y_1}^{\infty} dy_3 \cdot f_{A'_{c_1}A'_{c_2}A'_{c_3}}(y_1, y_2, y_3) \quad (19)$$

$$P_5 = \int_{0.5\cos\varphi_1}^{M\cos\varphi_1} dy_2 \int_{y_2}^{\infty} dy_1 \int_{y_2}^{\infty} dy_3 \cdot f_{A'_{c_1}A'_{c_2}A'_{c_3}}(y_1, y_2, y_3) \quad (20)$$

$$P_6 = \int_{0.5\cos\varphi_1}^{M\cos\varphi_1} dy_3 \int_{y_3}^{\infty} dy_1 \int_{y_3}^{\infty} dy_2 \cdot f_{A'_{c_1}A'_{c_2}A'_{c_3}}(y_1, y_2, y_3) \quad (21)$$

where

$$r' = \left(\frac{C}{I}\right)_{\mathrm{nom}} - r \quad (22)$$

$$x_t = \left\{\begin{aligned} &0.5\cos\varphi_1, && r' < 0.5 \\ &r'\cos\varphi_1, && 0.5 \le r' < M \\ &M\cos\varphi_1, && M \le r'. \end{aligned}\right. \quad (23)$$

For a balanced diversity system is assumed

$$\left(\frac{C}{I}\right)_{1,\,\mathrm{nom}} = \left(\frac{C}{I}\right)_{2,\,\mathrm{nom}} = \left(\frac{C}{I}\right)_{3,\,\mathrm{nom}} = \left(\frac{C}{I}\right)_{\mathrm{nom}}. \quad (24)$$

In the above expressions $f_{A'_{c_1}A'_{c_2}A'_{c_3}A'_{I_1}}(y_1, y_2, y_3, y_4)$, $f_{A'_{c_1}A'_{c_2}A'_{c_3}A'_{I_2}}(y_1, y_2, y_3, y_5)$, and $f_{A'_{c_1}A'_{c_2}A'_{c_3}A'_{I_3}}(y_1, y_2, y_3, y_6)$ are the joint density functions of the variables A'_{c_1}, A'_{c_2}, A'_{c_3}, A'_{I_1}, A'_{c_1}, A'_{c_2}, A'_{c_3}, A'_{I_2}, and A'_{c_1}, A'_{c_2}, A'_{c_3}, A'_{I_3}, respectively. Further $f_{A'_{c_1}A'_{c_2}A'_{c_3}}$ is the joint density function of the variables A'_{c_1}, A'_{c_2}, and A'_{c_3}. It should be noted that the same kind of joint probabilities also appear elsewhere [9], where the corresponding interference problem for a single-site system has been examined. In the present case, due to the complex geometry, the joint probabilities are much more complicated and consequently their reliable and accurate evaluation is the fundamental key of the whole analysis.

After using a straightforward statistical analysis, which is presented in Appendix B, the integrals of (16)–(21) can be

transformed to the following simplified forms:[1]

$$P_1 = \int_{u_{1k}}^{u_{1p}} du_1 \int_{u_1}^{\infty} du_2 \int_{u_1}^{\infty} du_3 f_{U_1U_2U_3}(u_1, u_2, u_3) \cdot \left[1 - \frac{1}{2}\operatorname{erfc}\left(\frac{u_{31} - \mu_4}{\sqrt{2}\sigma_4}\right)\right] \quad (25)$$

$$P_2 = \int_{u_{1k}}^{u_{1p}} du_2 \int_{u_2}^{\infty} du_1 \int_{u_2}^{\infty} du_3 f_{U_1U_2U_3}(u_1, u_2, u_3) \cdot \left[1 - \frac{1}{2}\operatorname{erfc}\left(\frac{u_{32} - \mu_5}{\sqrt{2}\sigma_5}\right)\right] \quad (26)$$

$$P_3 = \int_{u_{1k}}^{u_{1p}} du_3 \int_{u_3}^{\infty} du_1 \int_{u_3}^{\infty} du_2 f_{U_1U_2U_3}(u_1, u_2, u_3) \cdot \left[1 - \frac{1}{2}\operatorname{erfc}\left(\frac{u_{33} - \mu_6}{\sqrt{2}\sigma_6}\right)\right] \quad (27)$$

and

$$P_4 = \tfrac{1}{2} \int_{u_{oo}}^{u_{1p}} du_1 \int_{u_1}^{\infty} du_2 f_{U_1U_2}(u_1, u_2) \operatorname{erfc}\left(\frac{u_1 - \mu_3}{\sqrt{2}\sigma_3}\right) \quad (28)$$

$$P_5 = \tfrac{1}{2} \int_{u_{oo}}^{u_{1p}} du_2 \int_{u_2}^{\infty} du_3 f_{U_2U_3}(u_2, u_3) \operatorname{erfc}\left(\frac{u_2 - \mu_1}{\sqrt{2}\sigma_1}\right) \quad (29)$$

$$P_6 = \tfrac{1}{2} \int_{u_{oo}}^{u_{1p}} du_3 \int_{u_3}^{\infty} du_1 f_{U_1U_3}(u_1, u_3) \operatorname{erfc}\left(\frac{u_3 - \mu_2}{\sqrt{2}\sigma_2}\right) \quad (30)$$

where

$$u_{oo} = \frac{\ln(0.5 \cos \varphi_1) - \ln A_{m_1}}{S_{a_1}} \quad (31)$$

$$u_{1k} = \frac{\ln(x_t) - \ln A_{m_1}}{S_{a_1}} \quad (32)$$

$$u_{1p} = \frac{\ln(M \cos \varphi_1) - \ln A_{m_1}}{S_{a_1}} \quad (33)$$

$$u_{3j} = \frac{\ln\left[A_{m_1} e^{u_j S_{a_1}} \dfrac{\cos \varphi_2}{\cos \varphi_1} - r' \cos \varphi_2\right] - \ln A_{m_2}}{S_{a_2}}. \quad (34)$$

The analytical forms of the two-dimensional normal density functions $f_{U_1U_2}(u_1, u_2)$, $f_{U_2U_3}(u_2, u_3)$, and $f_{U_1U_3}(u_1, u_3)$ as well as the three-dimensional one $f_{U_1U_2U_3}(u_1, u_2, u_3)$ can be found in Appendix B.

The parameters μ_j, σ_j ($j = 1,2,3,4,5,6$) correspond to the proper conditional mean values and standard deviations in each case and are also presented in Appendix B.

In the above expressions A_{m_1} S_{a_1} are the lognormal statistical parameters of the attenuations A'_{c_1}, A'_{c_2}, and A'_{c_3} given by [16]

$$S_{a_1}^2 = \ell n\left[1 + \frac{H_{1c}}{L_{CD}^2}\left(\exp(b^2 S_r^2) - 1\right)\right] \quad (35)$$

$$A_{m_1} = a R_m^b L_{CD} \exp[(b^2 S_r^2 - S_{a_1}^2)/2]. \quad (36)$$

In addition, A_{m_2} and S_{a_2} are the lognormal statistical parameters of the attenuations A'_{I_1}, A'_{I_2}, or A'_{I_3} given by

$$S_{a_2}^2 = \ell n\left[1 + \frac{H_{1I}}{L_{ID}^2}\left(\exp(b^2 S_r^2) - 1\right)\right] \quad (37)$$

$$A_{m_2} = a R_m^b L_{ID} \exp[(b^2 S_r^2 - S_{a_2}^2)/2] \quad (38)$$

[1]The PASCAL code concerning the numerical calculation of the multidimensional integrals can be obtained by sending a request to the first author by e-mail at chvazour@cc.ece.ntua.gr.

in terms of the point rainfall parameters R_m, S_r the constants a and b of the specific attenuation and the factors H_{1C}, H_{1I} which have the form

$$H_{1X} = \begin{cases} 2L_{XD} G \sinh^{-1}\left(\dfrac{L_{XD}}{G}\right) + 2G^2\left[1 - \sqrt{1 + \left(\dfrac{L_{XD}}{G}\right)^2}\right], & \text{for } L_{XD} < D_r \\ 2L_{XD} G \sinh^{-1}\left(\dfrac{D_r}{G}\right) + 2G^2\left[1 - \sqrt{1 + \left(\dfrac{D_r}{G}\right)^2}\right] + \dfrac{G(L_{XD} - D_r)^2}{\sqrt{G^2 + D_r^2}}, & \text{for } L_{XD} \geq D_r \\ X = C, I \end{cases} \quad (39)$$

and G, D_r are characteristic parameters depending on the spatial structure of the rainfall medium [see also (15)].

Summarizing the procedure, the conditional probability under consideration (1)–(3) can be evaluated by means of the relationships (25)–(34). The lognormal statistical parameters A_{m_1}, S_{a_1} and A_{m_2}, S_{a_2} encountered in the previous relationships can be estimated by using (35)–(39). In addition, the statistical parameters μ_j, σ_j ($j = 1,2,3,4,5,6$) are expressed in terms of the logarithmic correlation coefficients $\rho_{n_{ij}}$ (i, $j = 1,2,3$, $i \neq j$) and $\rho_{n_{ik}}$ ($i = 1,2,3$; $k = 4,5,6$) which are evaluated in Appendixes B and C.

IV. Numerical Results and Discussion

We now proceed with the application of the preceding analysis to the prediction of differential rain attenuation induced by an adjacent path on a triple-site diversity system. A realistic communication system operating in Georgia and referring to the COMSTAR D_1 satellite [θ_{s_1} (geographical longitude) $= 128°$ W, $f = 19$ GHz] has been considered. In order to examine the performance of the interfered diversity system in association with the climatic zone, another communication system operating under analog conditions, but located in the tropical region (climatic zone Q) is also considered. The elevation angle φ_1 for the wanted satellite D_1 as seen from the earth stations located in Georgia is found to be 29°. The same value for φ_1 is also taken for the fictitious system operating somewhere in the tropical region. Implementation of the procedure requires knowledge of the parameters H, H_o, a, b, G, R_m, and S_r. A list of appropriate values for these parameters is presented in Table I. Some comments concerning their proper estimation are given here.

The effective rain height H is given by (6) using the geographical latitude of Georgia $\Lambda = 34°$. The location belonging to the Q climatic zone is considered to be in Brazil and corresponds to a geographical latitude $\Lambda = -40°$. The numerical values for the parameters a and b have been estimated by using the recent International Radio Consultative Committee (CCIR) report [15]. The estimation of the parameter G needs some more comments. The value $G = 1.75$

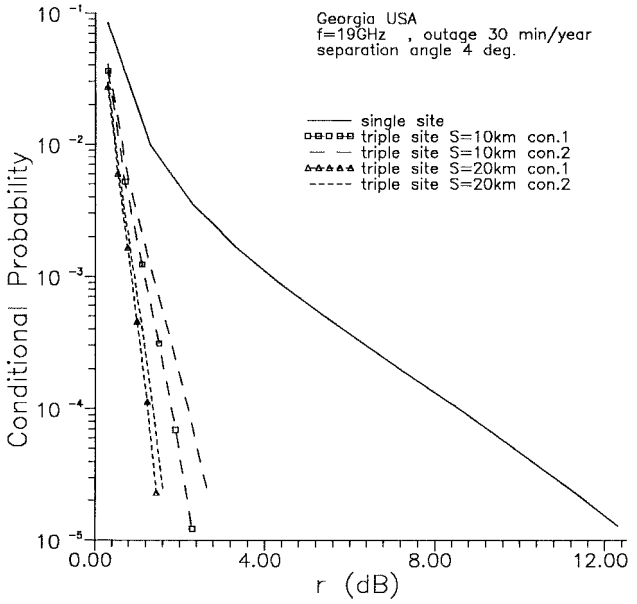

Fig. 2. Conditional probability versus attenuation level (r') for a single site and various cases of potentially existing triple-site diversity systems of different configuration and separation distance S. The other parameters are Location: Georgia, $f = 19$ GHz, $\varphi_1 = 29°$, and differential angle $\theta_d = 4°$ in the equatorial orbit.

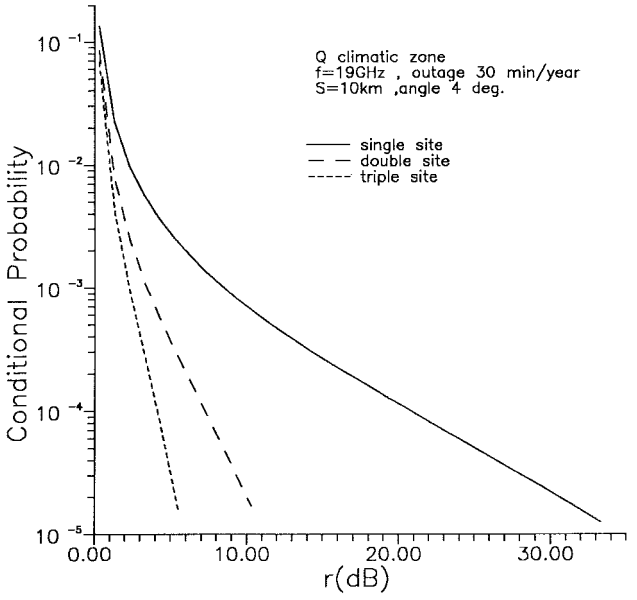

Fig. 3. Conditional probability versus attenuation level (r') for a single-site and the corresponding double- and triple-site diversity systems. The other parameters are Location: Q climatic zone, $f = 19$ GHz, $S = 10$ km, and $\theta_d = 4°$.

km has been selected as representative for the Georgia area because it gives a best fit to existing single-path and site-diversity attenuation data in this area [13]. On the other hand, the $G = 0.75$ km value is more suitable for tropical regions where high-intensity rainfalls of limited spatial extension is a usual phenomenon. As a final step, the lognormal parameters R_m and S_r are derived by means of a regression fitting technique implemented on the available rainfall data for the Georgia area [16] and the tropical climatic zone Q [14].

In Fig. 2, the conditional probability [expressed by (1)–(3)] is drawn versus r' for a single site and the corresponding triple-site interfered system, operating at the same rain attenuation outage time (30 min/yr in this case). Various cases of potentially existing site diversity systems are shown with separation distances $S = 10$ and 20 km [see Fig. 1(b)]. The geometrical setting of the three sites is a parameter of the whole problem and is examined analytically here. Configuration 1 is associated with arrangement of the stations in a straight line, whereas in configuration 2 the three sites form a triangle. The fictitious potential interfering satellite and the COMSTAR form a differential angle $\beta = 3.8°$ (in the equatorial orbit) in this case. The elevation angle φ_2, the angular separation θ_d and the projected differential angle $\Delta\Psi$ can be obtained by means of the β and the other geographical parameters of the problem as: $\varphi_2 = 29°$, $\theta_d = 4°$, and $\Delta\Psi = 4.3°$. The numerical values for φ_1, φ_2, and θ_d are also presented in Table I.

As may be seen the deviation of the triple-site diversity results in relation to the single-site ones is quite pronounced, even for small values of the separation distances (e.g., $S = 10$ km). On the other hand, there is a significant tendency of saturation for large values of S. Configuration 1 is concerned with the larger deviation. This is consistent with the smaller path correlation coefficients ρ_{ij} due to longer path ranges associated with this type of configuration.

In Fig. 3, a comparison of the triple-site interfered system with the respective double-site system operating at the same rain attenuation outage time, is attempted for a location belonging to the Q climatic zone. The other parameters of the problem are the same as before. As it is expected, the triple-site gives larger deviations in relation to the single site conditional probability results. Moreover, the latter probability takes quite significant values, even for small values of r' less than 10 dB.

Next, some more practical aspects of the whole problem are discussed. In Fig. 4, the differences $r'_s - r'_d/r'_s - r'_t$ between the differential attenuations for a single and the corresponding double-/triple-site diversity system versus the separation distance S are shown. In this case, three different locations of the potential interfering satellite are examined ($\theta_d = 4, 6,$ and $8°$) but φ_1 and φ_2 remain the same as above. The earth stations are cited in Georgia area. The following remarks can be deduced. First, the saturation of the differences $r'_s - r'_d/r'_s - r'_t$ for large values of S is clearly indicated, being a direct consequence of the previous considerations. As mentioned elsewhere [10], the differences $r'_s - r'_d/r'_s - r'_t$ are also equal to differences of the (C/I) ratio in decibels for the single and the respective double-/triple-site diversity system. In other words, they represent the "C/I diversity gain," a term analogous to the well established "diversity gain" referring to the (C/N) ratio used in this kind of problem. Another obvious remark, which can be deduced from this figure, is that the triple-site "C/I" diversity gain is always greater than the respective double-site one, their difference being more significant for large values of the differential angle ($\theta_d = 8°$) and for lower conditional probabilities (0.01% in the present case). On the other hand, the difference of $\ll C/I \gg$

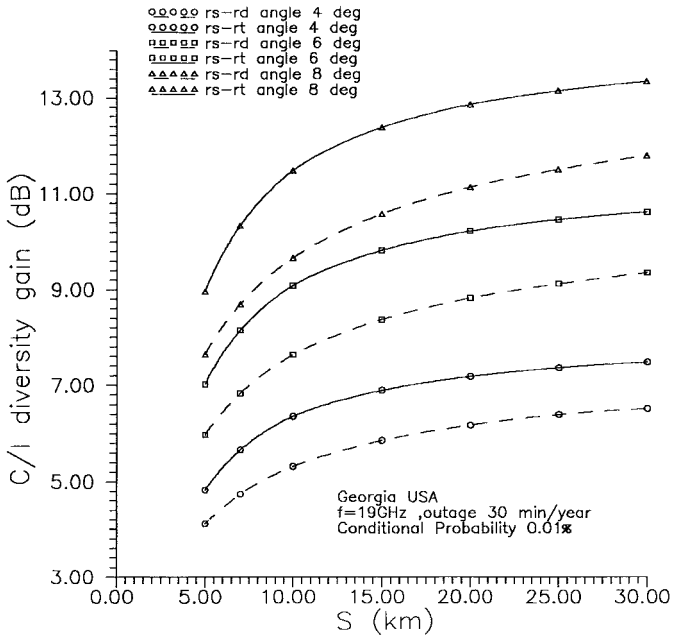

Fig. 4. "C/I" diversity gain versus separation distance S for a double-/triple-site diversity system in regard to the corresponding single site system for various differential angles $\theta_d = 4, 6,$ and $8°$. The other parameters are Location: Georgia, $f = 19$ GHz, conditional probability 0.01%.

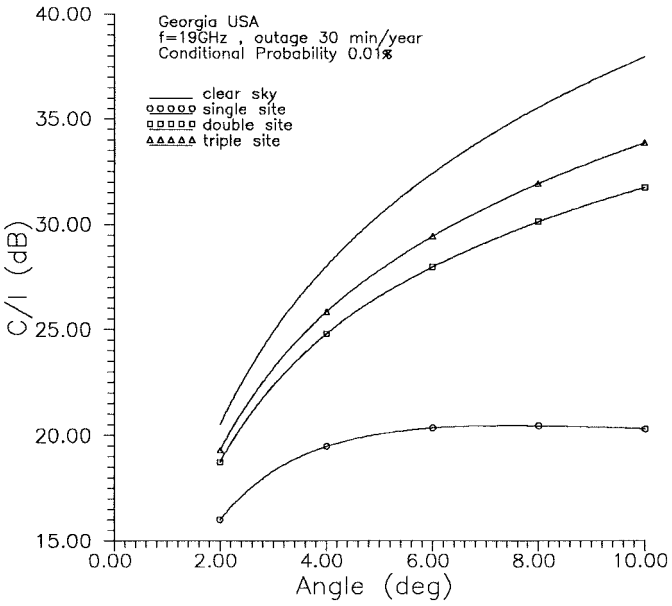

Fig. 5. Carrier-to-interference ratio (C/I) versus the angular separation θ_d, for a single site and the corresponding double-/triple-site diversity systems operating under the same rain-fade conditions. The other parameters are: Location: Georgia, $f = 19$ GHz, conditional probability: 0.01%.

diversity gains is always quite smaller than the respective value of the $\ll C/I \gg$ gain concerning the double-site system. Consequently, it seems to be a relatively little benefit to triple- over double-site diversity, but more about this matter will be discussed later.

Some other sets of curves which the system designer would like to see concern the effective carrier-to-interference (C/I) versus the angular separation θ_d of the two satellites. Following basic satellite link considerations [11], the (C/I) ratio of an earth-space system interfered by an adjacent satellite, under clear-sky conditions, is given by

$$\left(\frac{C}{I}\right)_{\text{nom}} = \text{EIRP}_s(\text{dBw}) - \text{EIRP}'_s(\text{dBw}) + G(\text{dB}) - (32 - 25\log\theta_d) \tag{40}$$

where EIRP_s is the equivalent isotropic radiated power of interfered satellite S_1 in the direction of interfered earth station E. Moreover, EIRP'_s is the equivalent isotropic radiated power of interfering satellite S_2 in the direction of interfered earth station E and G is the on-axis received antenna gain of the same station. The carrier-to-interference ratio under rain fading conditions is now expressed as

$$\left(\frac{C}{I}\right)(p\%) = \left(\frac{C}{I}\right)_{\text{nom}} - r'_s(p\%) \tag{41}$$

where p% is the percentage nonexceedance conditional probability and r'_s is the corresponding differential rain attenuation for the single-site system, under consideration.

In a similar way and assuming balanced diversity systems, the (C/I) of a multiple diversity system, with respect to a p% nonexceedance probability, can be expressed as

$$\left(\frac{C}{I}\right)(p\%) = \left(\frac{C}{I}\right)_{\text{nom}} - r'_d(p\%) \tag{42}$$

for double-site and

$$\left(\frac{C}{I}\right)(p\%) = \left(\frac{C}{I}\right)_{\text{nom}} - r'_t(p\%) \tag{43}$$

for triple-site diversity systems, respectively.

In Figs. 5 and 6, the $(C/I)(p\%)$ versus θ_d for an interfered system operating under the same specifications as before, using also double- and triple-site diversity protection are presented. As may be seen, the difference of (C/I) (in decibels) between a triple- and the corresponding double-site diversity with respect to the same differential angle is always quite small in comparison with the difference between the latter and the single-site system. This is in absolute agreement with the remark reported above concerning the relatively little benefit to triple- over double-site diversity.

On the other hand, one could argue that the need for using a triple-site diversity protection for a noise dominant system is imposed from the reduction of the very large possible fade margins. In addition, it can be observed that the relatively small difference of (C/I) results to a remarkable, in some cases, difference of angular separations between the satellites. This would be a very useful extract toward the establishment of the minimum separation between satellites operating under permitted interference levels.

To be more specific, we take as an example an interfered system located in Georgia (see Fig. 5). If our goal is the estimation of an upper angular threshold θ_{th}, so that the operating system violates the specified interference tolerance conditions, we can see the following.

For an allowed level less than 20 dB, the θ_{th} for the single-site system can be found to be less than 4° for 0.01% nonexceedance conditional probability, whereas the double and triple diversity protection systems give θ_{th} of the order of 2° and even more.

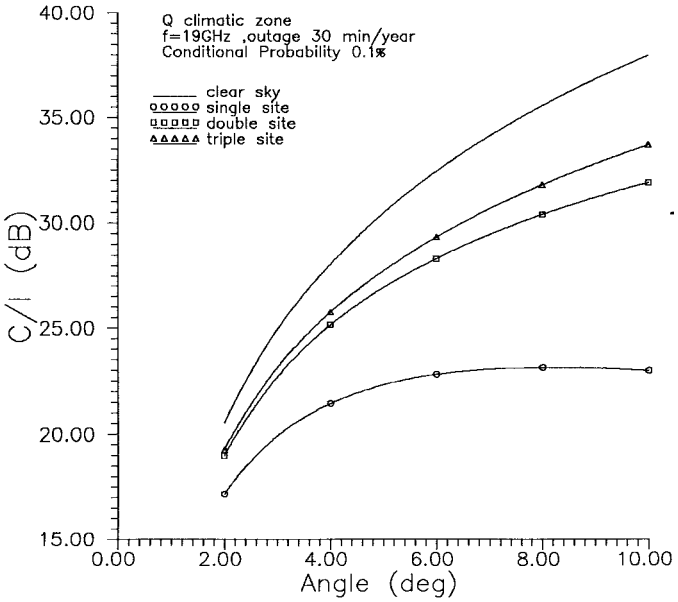

Fig. 6. The same as before but for Q climatic zone and conditional probability 0.1%.

For allowed levels greater than 20 dB, the single-site system presents values of θ_{th} much greater than 10°, while the $\theta_{th's}$ for the diversity protected systems range between 2–8°. More particularly, the effect of the triple in relation to the double-site system becomes more significant for allowed levels greater than 25 dB for the system under consideration. For example, for an allowed level of 28 dB, the θ_{th} for the double site can be found to be 6.5°, while the triple site gives 4.5°, yielding an angular difference of the order of 2°. This difference is estimated about 0.5°, in case the allowed level is 25 dB, leading for the triple-site system to a θ_{th} value of 3.6°.

In Fig. 6, numerical results for a similar interfered system located in the tropical region (climatic zone Q) are shown. All the above quantitative remarks seem to be valid but concerning a greater conditional nonexceedance probability (0.1% in this case). This is quite acceptable by taking into account that the tropical region is characterized by climatic zones of highest intensity rainfalls and limited spatial extension.

In conclusion, the triple-site diversity system although is imposed due to the necessity of reducing the large attenuation margins leads also to a significant, in some cases, reduction of the angular separation between the satellites without violating the imposed specifications for the permitted interference levels.

V. Conclusions

Differential rain attenuation is considered to be one of the main interference propagation effects between adjacent earth-space paths. In this paper, a previously developed systematic procedure for the prediction of differential rain attenuation, valid for single-/double-site systems, is properly modified to include the case the intended satellite signal is received by using a triple-site diversity protection scheme. The extended method is based on the convective rain cell model and is quite flexible to be applicable to any location of the world that the lognormal form for the rainfall distribution can be adopted. The numerical results refer to communication systems located in Georgia and somewhere in the tropical regions, taken as intended, for various locations of a fictitious potential interfering satellite. Some very useful remarks in the direction of a beneficial satellite design process can be deduced and are summarized here. A (C/I) diversity gain for the triple system is first defined. As may be observed, the triple-site (C/I) diversity gain is always greater than the respective double-site (C/I) gain, their difference being more significant for large values of the differential angle and for lower conditional probabilities.

Further, it seems to be a relatively little benefit to triple-site over double-site diversity in association with the observed difference of (C/I) gains. However, the examination of (C/I) versus θ_d diagrams reveals that the relatively small difference of (C/I) between a triple- and a double-site system, results generally to a remarkable difference of angular separation between the satellites.

As a general and aggregate conclusion, it can be deduced that although the triple-site diversity is imposed due to the necessity of reducing the very large attenuation margins, additive benefits could be provided. The angular separation reduction between satellites in geostationary orbit seems to be quite significant, in some cases, permitting the operation without violating the specified interference levels.

Appendix A
Derivation of the Expressions (1)–(3)

The output of the triple-site earth-space system is coming from the earth station with the least rain attenuation at each instant. The mathematical expression of this event is

$$\Omega = 0.5 < \min(A_{c_1}, A_{c_2}, A_{c_3}) < M. \tag{A.1}$$

It is clear that

$$\Omega = \Omega_1 \bigcup \Omega \bigcup \Omega_3 \tag{A.2}$$

where

$$\left.\begin{aligned} \Omega_1 &= (0.5 < A_{c_1} < M,\ A_{c_1} < A_{c_2},\ A_{c_1} < A_{c_3}) \\ \Omega_2 &= (0.5 < A_{c_2} < M,\ A_{c_2} < A_{c_1},\ A_{c_2} < A_{c_3}) \\ \Omega_3 &= (0.5 < A_{c_3} < M,\ A_{c_3} < A_{c_1},\ A_{c_3} < A_{c_2}) \end{aligned}\right\} \tag{A.3}$$

and

$$\Omega_i \bigcap \Omega_j = \emptyset \qquad i, j = 1, 2, 3,\ i \neq j. \tag{A.4}$$

Now, taking under consideration (A.2) and (A.4), one gets

$$P(\Omega) = P(\Omega_1) + P(\Omega_2) + P(\Omega_3). \tag{A.5}$$

During the occurrence of Ω_i event the whole system suffers by interference when $(C/I)_i < r,\ i = 1,2,3$. The latter probability can be formulated as

$$P_i = P\left(\left(\frac{C}{I}\right)_i < r,\ \Omega_i\right), \qquad i = 1, 2, 3. \tag{A.6}$$

As a result of the above, the percentage of the time that the triple-site system is interfered under the condition of operation

is

$$P = \frac{P_1 + P_2 + P_3}{P(\Omega_1) + P(\Omega_2) + P(\Omega_3)} \tag{A.7}$$

which is (1) of the main text.

APPENDIX B
EVALUATION OF THE PROBABILITIES IN EXPRESSIONS (16)–(21)

As pointed out in the main text, the joint exceedance probabilities under consideration can be calculated as

$$P_1 = \int_{x_t}^{M\cos\varphi_1} dy_1 \int_{y_1}^{\infty} dy_2 \int_{y_1}^{\infty} dy_3 \cdot \int_{o}^{(\cos\varphi_2/\cos\varphi_1)y_1 - r'\cos\varphi_2} \cdot f_{A'_{c_1}A'_{c_2}A'_{c_3}A'_{I_1}}(y_1, y_2, y_3, y_4)\, dy_4 \tag{B.1}$$

$$P_2 = \int_{x_t}^{M\cos\varphi_1} dy_2 \int_{y_2}^{\infty} dy_1 \int_{y_2}^{\infty} dy_3 \cdot \int_{o}^{(\cos\varphi_2/\cos\varphi_1)y_2 - r'\cos\varphi_2} \cdot f_{A'_{c_1}A'_{c_2}A'_{c_3}A'_{I_2}}(y_1, y_2, y_3, y_5)\, dy_5 \tag{B.2}$$

$$P_3 = \int_{x_t}^{M\cos\varphi_1} dy_3 \int_{y_3}^{\infty} dy_1 \int_{y_3}^{\infty} dy_2 \cdot \int_{o}^{(\cos\varphi_2/\cos\varphi_1)y_3 - r'\cos\varphi_2} \cdot f_{A'_{c_1}A'_{c_2}A'_{c_3}A'_{I_3}}(y_1, y_2, y_3, y_6)\, dy_6 \tag{B.3}$$

$$P_4 = \int_{0.5\cos\varphi_1}^{M\cos\varphi_1} dy_1 \int_{y_1}^{\infty} dy_2 \int_{y_1}^{\infty} dy_3 \cdot f_{A'_{c_1}A'_{c_2}A'_{c_3}}(y_1, y_2, y_3) \tag{B.4}$$

$$P_5 = \int_{0.5\cos\varphi_1}^{M\cos\varphi_1} dy_2 \int_{y_2}^{\infty} dy_1 \int_{y_2}^{\infty} dy_3 \cdot f_{A'_{c_1}A'_{c_2}A'_{c_3}}(y_1, y_2, y_3) \tag{B.5}$$

$$P_6 = \int_{0.5\cos\varphi_1}^{M\cos\varphi_1} dy_3 \int_{y_3}^{\infty} dy_1 \int_{y_3}^{\infty} dy_2 \cdot f_{A'_{c_1}A'_{c_2}A'_{c_3}}(y_1, y_2, y_3). \tag{B.6}$$

The parameter x_t in integrals (B.1)–(B.5) depends on the considered value of r' [see also (23)].

Adopting lognormal assumption (Section II) and using the following definition for the normal variables

$$\left.\begin{aligned} U_i &= \frac{\ln A'_{c_i} - \ln A_{m_1}}{S_{a_1}} \quad i = 1, 2, 3 \\ U_j &= \frac{\ln A'_{I_j} - \ln A_{m_2}}{S_{a_2}} \quad j = 4, 5, 6 \end{aligned}\right\} \tag{B.7}$$

we have

$$P_1 = \int_{u_{1k}}^{u_{1p}} du_1 \int_{u_1}^{\infty} du_2 \int_{u_1}^{\infty} du_3 \int_{-\infty}^{u_{31}} du_4 \cdot f_{U_1U_2U_3U_4}(u_1, u_2, u_3, u_4) \tag{B.8}$$

$$P_2 = \int_{u_{1k}}^{u_{1p}} du_1 \int_{u_2}^{\infty} du_2 \int_{u_2}^{\infty} du_3 \int_{-\infty}^{u_{32}} du_5 \cdot f_{U_1U_2U_3U_5}(u_1, u_2, u_3, u_5) \tag{B.9}$$

$$P_3 = \int_{u_{1k}}^{u_{1p}} du_3 \int_{u_3}^{\infty} du_1 \int_{u_3}^{\infty} du_2 \int_{-\infty}^{u_{33}} du_6 \cdot f_{U_1U_2U_3U_6}(u_1, u_2, u_3, u_6) \tag{B.10}$$

$$P_4 = \int_{u_{00}}^{u_{1p}} du_1 \int_{u_1}^{\infty} du_2 \int_{u_1}^{\infty} du_3 \cdot f_{U_1U_2U_3}(u_1, u_2, u_3) \tag{B.11}$$

$$P_5 = \int_{u_{00}}^{u_{1p}} du_2 \int_{u_2}^{\infty} du_1 \int_{u_2}^{\infty} du_3 \cdot f_{U_1U_2U_3}(u_1, u_2, u_3) \tag{B.12}$$

$$P_6 = \int_{u_{00}}^{u_{1p}} du_3 \int_{u_3}^{\infty} du_1 \int_{u_3}^{\infty} du_2 \cdot f_{U_1U_2U_3}(u_1, u_2, u_3). \tag{B.13}$$

The definition of u_{1k}, u_{1p}, u_{oo}, u_{3j} is given in the main text.

Now using the Bayes theorem, the joint density functions $f_{U_1U_2U_3U_4}$, $f_{U_1U_2U_3U_5}$, $f_{U_1U_2U_3U_6}$, $f_{U_1U_2U_3}$ can be expressed as

$$f_{U_1U_2U_3U_k}(u_1, u_2, u_3, u_k) = f_{U_1U_2U_3}(u_1, u_2, u_3) f_{U_k/U_1U_2U_3}(u_1, u_2, u_3) \qquad k = 4, 5, 6 \tag{B.14}$$

$$\begin{aligned} f_{U_1U_2U_3}(u_1, u_2, u_3) &= f_{U_1U_2}(u_1, u_2) f_{U_3/U_1U_2}(u_1, u_2) \\ &= f_{U_2U_3}(u_2, u_3) f_{U_1/U_2U_3}(u_2, u_3) \\ &= f_{U_1U_3}(u_1, u_3) f_{U_2/U_1U_3}(u_1, u_3). \end{aligned} \tag{B.15}$$

Substituting (B.14)–(B.15) into (B.8)–(B.13) and using the following result from the theory of normal variables:

$$\int_A^B f(x)\, dx = \frac{1}{2}\left[\operatorname{erfc}\left(\frac{A-m}{\sqrt{2\sigma}}\right) - \operatorname{erfc}\left(\frac{B-m}{\sqrt{2\sigma}}\right)\right] \tag{B.16}$$

where $f(x)$ is a normal density function with parameters (m, σ), one gets (25)–(30) of the main text.

The joint density functions $f_{U_1U_2}$, $f_{U_2U_3}$, $f_{U_1U_3}$, $f_{U_1U_2U_3}$ encountered in (25)–(30), as well as the analytical forms for μ_j, σ_j $(j = 1,2,3,4,5,6)$ can be defined as [12]

$$f_{U_iU_j}(u_i, u_j) = \frac{1}{2\pi\sqrt{1-\rho_{n_{ij}}^2}} \exp\left[-\frac{u_i^2 + u_j^2 - 2\rho_{n_{ij}}u_iu_j}{2(1-\rho_{n_{ij}}^2)}\right] \qquad (i, j = 1, 2, 3, i \neq j) \tag{B.17}$$

$$f_{U_1U_2U_3} = \frac{1}{\sqrt{(2\pi)^3 D}} \exp\left[-\frac{1}{2} Z(u_1, u_2, u_3)\right] \tag{B.18}$$

$$\left.\begin{aligned} \mu_1 &= \frac{\rho_{n_{12}} - \rho_{n_{13}}\rho_{n_{23}}}{1-\rho_{n_{23}}^2} u_2 + \frac{\rho_{n_{13}} - \rho_{n_{23}}\rho_{n_{12}}}{1-\rho_{n_{23}}^2} u_3 \\ \sigma_1^2 &= \frac{D}{1-\rho_{n_{23}}^2} \end{aligned}\right\} \tag{B.19}$$

$$\left.\begin{aligned} \mu_2 &= \frac{\rho_{n_{12}} - \rho_{n_{13}}\rho_{n_{23}}}{1-\rho_{n_{13}}^2} u_1 + \frac{\rho_{n_{23}} - \rho_{n_{12}}\rho_{n_{13}}}{1-\rho_{n_{13}}^2} u_3 \\ \sigma_2^2 &= \frac{D}{1-\rho_{n_{13}}^2} \end{aligned}\right\} \tag{B.20}$$

$$\left.\begin{aligned}\mu_3 &= \frac{\rho_{n_{13}} - \rho_{n_{12}}\rho_{n_{23}}}{1-\rho_{n_{12}}^2}\,u_1 + \frac{\rho_{n_{23}} - \rho_{n_{12}}\rho_{n_{13}}}{1-\rho_{n_{12}}^2}\,u_2 \\ \sigma_3^2 &= \frac{D}{1-\rho_{n_{12}}^2}\end{aligned}\right\} \quad \text{(B.21)}$$

$$D = 1 - \rho_{n_{12}}^2 - \rho_{n_{23}}^2 - \rho_{n_{13}}^2 + 2\rho_{n_{12}}\rho_{n_{23}}\rho_{n_{13}} \quad \text{(B.22)}$$

$$Z(u_1, u_2, u_3) = \frac{1}{D}[A_{11}u_1^2 + A_{22}u_2^2 + A_{33}u_3^2 + 2A_1A_2u_1u_2 + 2A_{13}u_1u_3 + 2A_{23}u_2u_3] \quad \text{(B.23)}$$

$$\left.\begin{aligned}A_{11} &= 1 - \rho_{n_{23}}^2 \\ A_{12} &= A_{21} = \rho_{n_{13}}\rho_{n_{23}} - \rho_{n_{12}} \\ A_{13} &= A_{31} = \rho_{n_{12}}\rho_{n_{23}} - \rho_{n_{13}} \\ A_{22} &= 1 - \rho_{n_{13}}^2 \\ A_{23} &= A_{32} = \rho_{n_{12}}\rho_{n_{13}} - \rho_{n_{23}} \\ A_{33} &= 1 - \rho_{n_{12}}^2\end{aligned}\right\} \quad \text{(B.24)}$$

$$\mu_k = E\{u_k/u_1, u_2, u_3\} = a_{1k}u_1 + a_{2k}u_2 + a_{3k}u_3 \quad \text{(B.25)}$$

$$\sigma_k^2 = 1 - Z(\rho_{n_{1k}}, \rho_{n_{2k}}, \rho_{n_{3k}}) \quad \text{(B.26)}$$

$$\left.\begin{aligned}a_{1k} &= \frac{A_{11}\rho_{n_{1k}} + A_{12}\rho_{n_{2k}} + A_{13}\rho_{n_{3k}}}{D} \\ a_{2k} &= \frac{A_{12}\rho_{n_{1k}} + A_{22}\rho_{n_{2k}} + A_{23}\rho_{n_{3k}}}{D} \\ a_{3k} &= \frac{A_{13}\rho_{n_{1k}} + A_{23}\rho_{n_{2k}} + A_{33}\rho_{n_{3k}}}{D}\end{aligned}\right\} \quad (k = 4, 5, 6). \quad \text{(B.27)}$$

In the above expressions, $\rho_{n_{12}}$ is the correlation coefficient between $\ln A'_{c_1}$, $\ln A'_{c_2}$, $\rho_{n_{23}}$ between $\ln A'_{c_2}$, $\ln A'_{c_3}$, and $\rho_{n_{31}}$ between $\ln A'_{c_3}$, $\ln A'_{c_1}$ given by [9]

$$\rho_{n_{ij}} = \frac{\ell n\left[1 + \rho_{ij}\left(e^{S_{a_1}^2} - 1\right)\right]}{S_{a_1}^2} \qquad (i, j = 1, 2, 3,\ i \neq j) \quad \text{(B.28)}$$

in terms of the path correlation coefficients ρ_{ij} between the same attenuations A'_{c_1}, A'_{c_2}, and A'_{c_3}.

The path correlation coefficient ρ_{ij} can be expressed as

$$\rho_{ij} = \frac{H_{ij}}{H_{1C}} \quad \text{(B.29)}$$

where the factor H_{ij} has been evaluated elsewhere [10] and, consequently, the results are only presented here

$$H_{ij} = \int_{K_{ij}-L_{CD}}^{K_{ij}} (L_{CD} - K_{ij} + x)\rho(d_{ij})\,dx + \int_{K_{ij}}^{L_{CD}+K_{ij}} (L_{CD} + K_{ij} - x)\rho(d_{ij})\,dx \quad \text{(B.30)}$$

$$d_{ij} = \sqrt{D_{ij}^2 + x^2} \quad \text{(B.31)}$$

$$K_{ij} = \sqrt{S_{ij}^2 - D_{ij}^2} \quad \text{(B.32)}$$

and $\rho(d_{ij})$ is the correlation coefficient between the rainfall rates with respect to points been at a distance d_{ij} [see Fig. 1(b)], and given in (15) of the main text. Moreover, D_{ij} is the distance between the projected slant radio paths E_iS_1 and E_jS_1 [see also Fig. 1(b)].

In the same way, $\rho_{n_{14}}$ is the correlation coefficient between $\ln A'_{c_1}$, $\ln A'_{I_1}$, $\rho_{n_{24}}$ between $\ln A'_{c_2}$, $\ln A'_{I_1}$, and $\rho_{n_{34}}$ between $\ln A'_{c_3}$, $\ln A'_{I_1}$. The same holds for the $\rho_{n_{15}}$, $\rho_{n_{25}}$, $\rho_{n_{35}}$ and $\rho_{n_{16}}$, $\rho_{n_{26}}$, $\rho_{n_{36}}$ correlating the $\ln A'_{c_1}$, $\ln A'_{c_2}$, $\ln A'_{c_3}$ with the $\ln A'_{I_2}$ and $\ln A'_{I_3}$ variables, respectively. The above correlation coefficients are given by the general formula

$$\rho_{n_{ik}} = \frac{\ell n\left[1 + \rho_{ik}\sqrt{\left(e^{S_{a_1}^2} - 1\right)\left(e^{S_{a_1}^2} - 1\right)}\right]}{S_{a_1}.S_{a_2}} \qquad (i = 1, 2, 3 \text{ and } k = 4, 5, 6) \quad \text{(B.33)}$$

in terms of the corresponding path correlation coefficients ρ_{ik}. The latter coefficients can also be expressed as [10]

$$\rho_{ik} = \frac{H_{ik}}{\sqrt{H_{1C}.H_{1I}}}. \quad \text{(B.34)}$$

Analytical presentation of the factors H_{ik} can be found in Appendix C.

Appendix C
Factors H_{ik}

Following their definitions the factors H_{ik} ($i = 1,2,3$, $k = 4,5,6$) can be defined as follows [see Fig. 1(c)]:

$$H_{14} = \int_o^{L_{CD}} dz \int_o^{L_{ID}} dz'\rho(z, z') \quad \text{(C.1)}$$

$$H_{24} = \int_{D_{12}^{(1)}}^{D_{12}^{(1)}+L_{ID}} dz' \int_{D_{12}^{(2)}}^{D_{12}^{(2)}+L_{CD}} dz\rho(z, z') \quad \text{(C.2)}$$

$$H_{34} = \int_{D_{13}^{(1)}}^{D_{13}^{(1)}+L_{ID}} dz' \int_{D_{13}^{(2)}}^{D_{13}^{(2)}+L_{CD}} dz\rho(z, z') \quad \text{(C.3)}$$

$$H_{15} = \int_{D_{12}^{(3)}}^{D_{12}^{(3)}+L_{ID}} dz' \int_{D_{12}^{(4)}}^{D_{12}^{(4)}+L_{CD}} dz\rho(z, z') \quad \text{(C.4)}$$

$$H_{25} = \int_o^{L_{CD}} dz \int_o^{L_{ID}} dz'\rho(z, z') \quad \text{(C.5)}$$

$$H_{35} = \int_{D_{23}^{(1)}}^{D_{23}^{(1)}+L_{ID}} dz' \int_{D_{23}^{(2)}}^{D_{23}^{(2)}+L_{CD}} dz\rho(z, z') \quad \text{(C.6)}$$

$$H_{16} = \int_{D_{13}^{(3)}}^{D_{13}^{(3)}+L_{ID}} dz' \int_{D_{13}^{(4)}}^{D_{13}^{(4)}+L_{CD}} dz\rho(z, z') \quad \text{(C.7)}$$

$$H_{26} = \int_{D_{23}^{(3)}}^{D_{23}^{(3)}+L_{ID}} dz' \int_{D_{23}^{(4)}}^{D_{23}^{(4)}+L_{CD}} dz\rho(z, z') \quad \text{(C.8)}$$

and

$$H_{36} = \int_o^{L_{CD}} dz \int_o^{L_{ID}} dz'\rho(z, z') \quad \text{(C.9)}$$

where $\rho(z, z')$ denotes the spatial correlation function and is a function of the distance $d(z, z') = \sqrt{z^2 + z'^2 - 2zz'\cos\Delta\Psi}$ between two points belonging to the projections of the slant paths under consideration, whereas $\Delta\Psi$ is the projected differential angle.

The lengths $D_{ij}^{(\ell)}$ ($i = 1,2$, $j = 2,3$,$i < j$, $\ell = 1,2,3,4$) are given by the following expressions:

$$\left.\begin{aligned} D_{ij}^{(1)} &= \frac{D_{ij}}{\sin \Delta\Psi} - L_{ID} \\ D_{ij}^{(2)} &= \frac{D_{ij}}{\tan \Delta\Psi} - L_{CD} + K_{ij} \\ D_{ij}^{(3)} &= \frac{D_{ij}}{\sin \Delta\Psi} \\ D_{ij}^{(4)} &= \frac{D_{ij}}{\tan \Delta\Psi} + K_{ij} \end{aligned}\right\} \qquad \text{(C.10)}$$

where ω_{ij} is the orientation angle between E_i and E_j earth-terminal stations [see Fig. 1(d) for $\omega_{ij} < 90°$ and Fig. 1(e) for $\omega_{ij} > 90°$].

REFERENCES

[1] D. D. Tang, D. Davidson, and S. C. Bloch, "Diversity reception of Comstar satellite 19/29 GHz beacons with the Tampa triad," *Radio Sci. (1978–1981)*, vol. 17, pp. 1477–1488, 1982.

[2] D. C. Hogg, "Path diversity in propagation of millimeter waves through rain," *IEEE Trans. Antennas Propagat.*, vol. AP-15, pp. 410–415, 1967.

[3] D. B. Hodge, "Path diversity for reception of satellite signals," *J. Res. Atmosph..*, vol. 8, pp. 443–449, 1974.

[4] J. E. Allnutt and D. V. Rogers, "Novel method for predicting site diversity gain on satellite to ground radio paths," *Electron. Lett.*, vol. 18, pp. 233–235, 1982.

[5] J. E. Allnutt, "Nature of space diversity in microwave communications via geostationary satellites: A review," *Proc. Inst. Elect. Eng.*, vol. 125, pp. 369–376, May 1978.

[6] J. Goldhirsh and B. H. Musiani, "Two years of three site diversity measurements at 20 GHz with ACTS," in *North Amer. Radio Sci. Meet.*, Montreal, Canada, July 1997.

[7] R. R. Rogers, R. L. Olsen, J. I. Strickland, and G. M. Coulson, "Statistics of differential rain attenuation on adjacent earth–space propagation paths," *Ann. Telecommun.*, vol. 37, nos. 11/12, pp. 445–452, 1982.

[8] J. D. Kanellopoulos and V. A. Houdzoumis, "A model for the prediction of differential rain attenuation on adjacent earth-space propagation paths," *Radio Sci.*, vol. 25, no. 5, pp. 853–864, 1990.

[9] J. D. Kanellopoulos, S. Ventouras, and C. N. Vazouras, "A revised model for the prediction of differential rain attenuation on adjacent earth-space propagation paths," *Radio Sci.*, vol. 28, no. 6, pp. 1071–1086, 1993.

[10] J. D. Kanellopoulos and S. Ventouras, "Analysis of the interference due to differential rain attenuation induced by an adjacent path on a dual site diversity earth-space system," *Radio Sci.*, vol. 31, no. 6, pp. 1435–1448, 1996.

[11] T. T. Ha, *Digital Satellite Communications.* New York: Macmillan, 1986, p. 573.

[12] A. Papoulis, *Random Variables and Stochastic Processes.* New York: McGraw-Hill, 1965.

[13] J. D. Kanellopoulos and S. G. Koukoulas, "Prediction of triple-site diversity performance in earth-space communication," *J. Elect. Waves Applicat.*, vol. 4, no. 4, pp. 341–358, 1990.

[14] R. K. Crane, "Prediction of attenuation by rain," *IEEE Trans. Commun.*, vol. COM-28, pp. 1717–1733, Sept. 1980.

[15] CCIR, "Propagation data and prediction methods required for earth-space communication systems," *Int. Telecommun.*, Rep. 564-2 (MOD F), Doc. 5/1040-E, Union, Geneva, Switzerland, 1985.

[16] S. H. Lin, "A method for calculating rain attenuation distribution on microwave paths," *Bell Syst. Tech. J.*, vol. 54, no. 6, pp. 1051–1086, 1975.

[17] J. D. Kanellopoulos and S. G. Koukoulas, "Analysis of rain outage performance of roule diversity systems," *Radio Sci.*, vol. 22, no. 4, pp. 549–565, 1987.

John D. Kanellopoulos (SM'90) was born in Athens, Greece, on December 12, 1948. He received the Dipl. Electrical Engineering in 1971 and the Dr.Eng. degrees from the National Technical University of Athens (NTUA), Greece, in 1971 and 1979, respectively, and the D.I.C. and Ph.D. degrees from the Imperial College of Science, Technology, and Medicine, University of London, U.K., in 1979.

In November 1979, he joined the Department of Electrical Engineering, NTUA, where he is now a Professor.

Dr. Kanellopoulos is a member of IEICE, Optimal Society of America, New York Academy of Science, and the Massachusetts Institute of Technology (MIT) Electromagnetics Academy, Cambridege, MA. He has also received a number of awards and honors from the American Biographical Institute and International Biographical Center.

Spiros N. Livieratos was born in Athens, Greece, on February 22, 1969. He received the Dipl. of Electrical and Computer Engineering and the Dr.Eng. degree from the National Technical University of Athens (NTUA), Greece, in 1992 and 1998, respectively. He is currently working toward the Executive M.Sc. in Business Administration from the Economic University of Athens while serving in the forces of the Hellenic Navy.

His research interests include microwave communications and digital satellite communication systems.